Journal of
Marine Science and Engineering

MDPI

Review

Ocean Fronts and Their Acoustic Effects: A Review

Yuyao Liu, Zhou Meng, Wen Chen, Yan Liang, Wei Chen * and Yu Chen *

College of Meteorology and Oceanography, National University of Defense Technology, Changsha 410073, China
* Correspondence: kevinkobegames@126.com (W.C.); chenyu@nudt.edu.cn (Y.C.)

Abstract: As one of the widespread physical phenomena in the global ocean system, the ocean front has a very important influence on underwater sound propagation. Firstly, this paper systematically reviews several methods for the detection of ocean fronts in the past decades, including traditional oceanographic methods, artificial intelligence methods, and acoustic methods, highlighting the advantages and disadvantages of each method. Next, some modeling studies of ocean fronts are reported in this paper. Based on the above research, we pay more attention to research progress on the acoustic effects of ocean fronts, including simulation analysis and experimental research, which has also been the focus of underwater acousticians for a long time. In addition, this paper looks forward to the future development direction of this field, which can provide good guidance for the study of ocean fronts and their acoustic effects in the future.

Keywords: ocean front; acoustic effect; detecting method; sound speed profile (SSP); modeling; experiment

check for updates

Citation: Liu, Y.; Meng, Z.; Chen, W.; Liang, Y.; Chen, W.; Chen, Y. Ocean Fronts and Their Acoustic Effects: A Review. *J. Mar. Sci. Eng.* **2022**, *10*, 2021. https://doi.org/10.3390/jmse10122021

Academic Editor: Anatoly Gusev

Received: 23 November 2022
Accepted: 14 December 2022
Published: 17 December 2022

1. Introduction

The study of physical phenomena at various scales in the global ocean system is becoming a hot topic in oceanography. These physical phenomena exist widely in the global oceans and often have a certain periodicity. The common physical phenomena mainly include mesoscale vortexes (named eddies) [1], internal waves [2], and ocean fronts [3]. Due to complex ocean currents or water masses [4] and the undulating seafloor topography [5], there are many ocean fronts with different properties and intensities in the ocean system. In the context of physical oceanography, the ocean front is defined as a narrow transitional zone between two or several water masses with different properties [3]. In the frontal area, many environmental parameters change drastically, and there is strong mixing exchange, convergence (divergence), and vertical movement, which have important effects on underwater sound propagation [6], underwater target detection [7], pollutants dynamics [8], and maritime search and rescue activities. Among them, the study of the influence of the ocean front on underwater sound propagation has become the focus of underwater acousticians [9–13].

In recent years, with the rapid development of satellite observations, numerical models, acoustic theoretical models, and marine survey experiments, numerous new methods have emerged to study typical ocean phenomena, such as ocean fronts and their acoustic effects. It is necessary to systematically summarize and report these new methods to provide more references in the future. In fact, a few previous studies tend to neglect some specific links in the whole process of ocean fronts and their acoustic effects due to different emphases. For example, acoustic experiments may not attach importance to the detection of the ocean front, or the simulation analysis of the ocean front acoustic effects do not have enough experimental data as support, which makes the research process incomplete. Therefore, it is essential for us to summarize the research methods of each link in the whole research process, to provide good guidance for future comprehensive research in this field.

In this paper, ocean fronts and their acoustic effects are studied. The whole research process is summarized, and the technical route is given in Figure 1. Firstly, the detection methods of ocean fronts in recent decades are reviewed, including traditional oceanographic methods, artificial intelligence methods, and detection methods based on sound speed profile (SSP). Next, this paper reports some theoretical modeling studies of ocean fronts, including oceanographic modeling and sound speed field modeling for acoustic effect study. Then, the theoretical and experimental research progresses on the acoustic effects of ocean fronts are reported. Finally, this paper summarizes and prospects the development direction of this field in the future. Unlike previous reviews, in this review, we focus on the acoustic effects of ocean fronts. Therefore, from all aspects of the ocean front research process, including the detection of ocean fronts (Section 2.2), ocean front modeling (Section 3), and so on, we separate reported acoustic methods from traditional methods. At the same time, we review the research progress on the acoustic effects of ocean fronts (Section 4), to highlight the attention paid to the acoustic effects of ocean fronts.

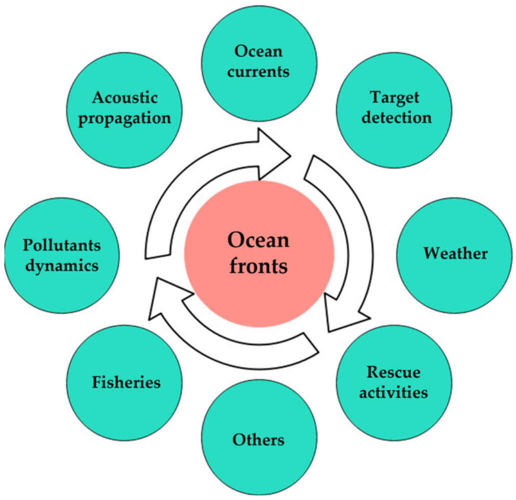

Figure 1. Influences of the ocean front in the world's oceanic and atmospheric environment.

2. Definition and Detection Method of the Ocean Front

2.1. Definition of the Ocean Front

The ocean front is a narrow zone of enhanced horizontal gradients of seawater properties (temperature, salinity, sound speed, nutrients, and so on) that separates broader areas with different water masses or different vertical structures (stratification) [14]. The ocean front plays an important role in the world's oceanic and atmospheric environment (Figure 1). Ocean fronts are often described as discontinuous because of their abruptness, which occurs over a range of lengths, from a few meters to thousands of kilometers. Ocean fronts may be transient (a few days), although most are quasi-stationary and seasonally persistent; the protruding front is present all year round. The difference in sea surface temperature and sea surface salinity across the front can be as large as 10–15 °C and 2–3 parts per thousand (ppt), respectively, with a typical difference of 2–5 °C and 0.3–1.0 ppt. The vertical range of the ocean front is from a few meters to more than a kilometer, with major ocean fronts reaching the open ocean bottom at depths exceeding 4 km [3].

In the context of physical oceanography, the types of ocean fronts are different due to differences in the physical processes that form them, such as estuarine, plume, and coastal buoyancy current fronts; mid-shelf fronts; tidal mixing fronts; coastal, topographic, and equatorial upwelling fronts; shelf-slope/shelf break fronts; western and eastern boundary current fronts; marginal ice zone fronts; subtropical convergence fronts, and water mass fronts [15]. These ocean fronts also have chemical and biological manifestations. As a rule, an ocean front in one property can be detected in other properties. For example, temperature fronts are almost always associated with sound speed fronts since seawater sound speed is a function of temperature, salinity, and pressure (depth). Major fronts are associated with fronts in other properties, such as nutrients, ocean color, chlorophyll, and turbidity. The concurrent physical, chemical, and biological manifestations of the same front are typically collocated, although relatively minor spatial offsets have been observed between locations of the same fronts in different properties. As an important factor affecting the characteristics of underwater sound propagation, the SSP reflects the vertical distribution structure of the seawater sound speed [16–19]. Due to the drastic changes in temperature and other environmental parameters, the SSP in the sea area where the ocean front exists will also have drastic changes [11,20,21]. The presence of an ocean front changes the structure of the SSP at a certain distance and depth, which will have a great impact on underwater sound propagation.

2.2. Detection Methods of the Ocean Front

2.2.1. Traditional Oceanographic Methods

During the last several decades, there has been significant advancement of our accrued knowledge and understanding of oceanographic phenomenology, circulation, and variability in global and specific regional oceans. It is important to recognize the role of ocean fronts in describing regional circulation. Figure 2 shows the distribution of main ocean fronts in some global sea areas according to [3]. From a regional modeling and prediction perspective, the identification of an ocean front may be associated with different processes relevant to the local regional dynamics and phenomenology. For example, a large-scale Gulf Stream meandering frontal system also defines the boundaries of unique water masses, which, in turn, defines the boundary of the basin and sub-basin-scale gyres in a synoptic state [22]. With the continuous development of satellite technology and numerical models, many real-time remote sensing data of the global surface ocean, combined with increasingly mature numerical model results with high spatial and temporal resolution and a large range of on-site observation data, the research on the spatiotemporal detection and evolution mechanism of global ocean fronts has gradually become one of the hot spots in physical oceanography. There are several methods of detecting ocean fronts from satellite data and images, using the gradient [23,24], cluster-shade algorithms [25], or histogram algorithms [26,27]. In the world's oceans, Kahru et al. [28], Moore et al. [29], Ullman and Cornillon [30,31], Kostianoy et al. [32], and Park et al. [33], used satellite remote sensing sea surface temperature (SST) data to study the ocean front in the Baltic Sea, the Antarctic, the Pacific Ocean and its coasts, the South Indian Ocean, and the Japan Sea, respectively. Hickox et al. [34] used Pathfinder SST data set (https://www.nodc.noaa.gov/satellitedata/pathfinder4km53/ (accessed on 1 October 2022)) from 1985 to 1996 to study the sea surface temperature fronts in the East China, Yellow, and Bohai Seas and defined 10 sea surface temperature fronts that generally exist in the study area. Wang et al. [35] analyzed the distribution positions and seasonal changes of several major fronts in the north of the South China Sea by calculating the frequency of front occurrence using the multi-year monthly average satellite remote sensing SST data. Chu et al. [36] studied the seasonal change of the South China Sea front using the GDEM (Generalized Digital Environmental Model) climate state data set, and pointed out that there is a front in the northern continental shelf area of the South China Sea along the east coast of Vietnam to Luzon Island in the Philippines; the maximum gradient of the front is 50 m above the current subsurface. Chen [37] summarized the achievements of predecessors and systematically summarized the ocean front existing on the surface/underwater in the Bohai Sea, the Yellow Sea, and the East China Sea, using satellite data and open data. Zhu et al. [38] analyzed the mixing characteristics of the Subarctic Front (SAF) in the Kuroshio-Oyashio confluence region based on temperature, salinity, and current data obtained from surveys and remote sensing.

From the perspective of oceanography, the traditional method of detecting ocean front is the most intuitive and has broad significance, but it should be noted that the frontal zone detected can sometimes contain too many spikes and become chaotic, leading to a negative effect for visual interpretation. Additionally, most conventional methods that focus on extracting the ridges of fronts struggle with false fronts due to imperfect data. Further, choosing appropriate thresholds for them is another dilemma, which sometimes leads to too many frontal ridges in unwanted areas or too little than needed in the region of interest.

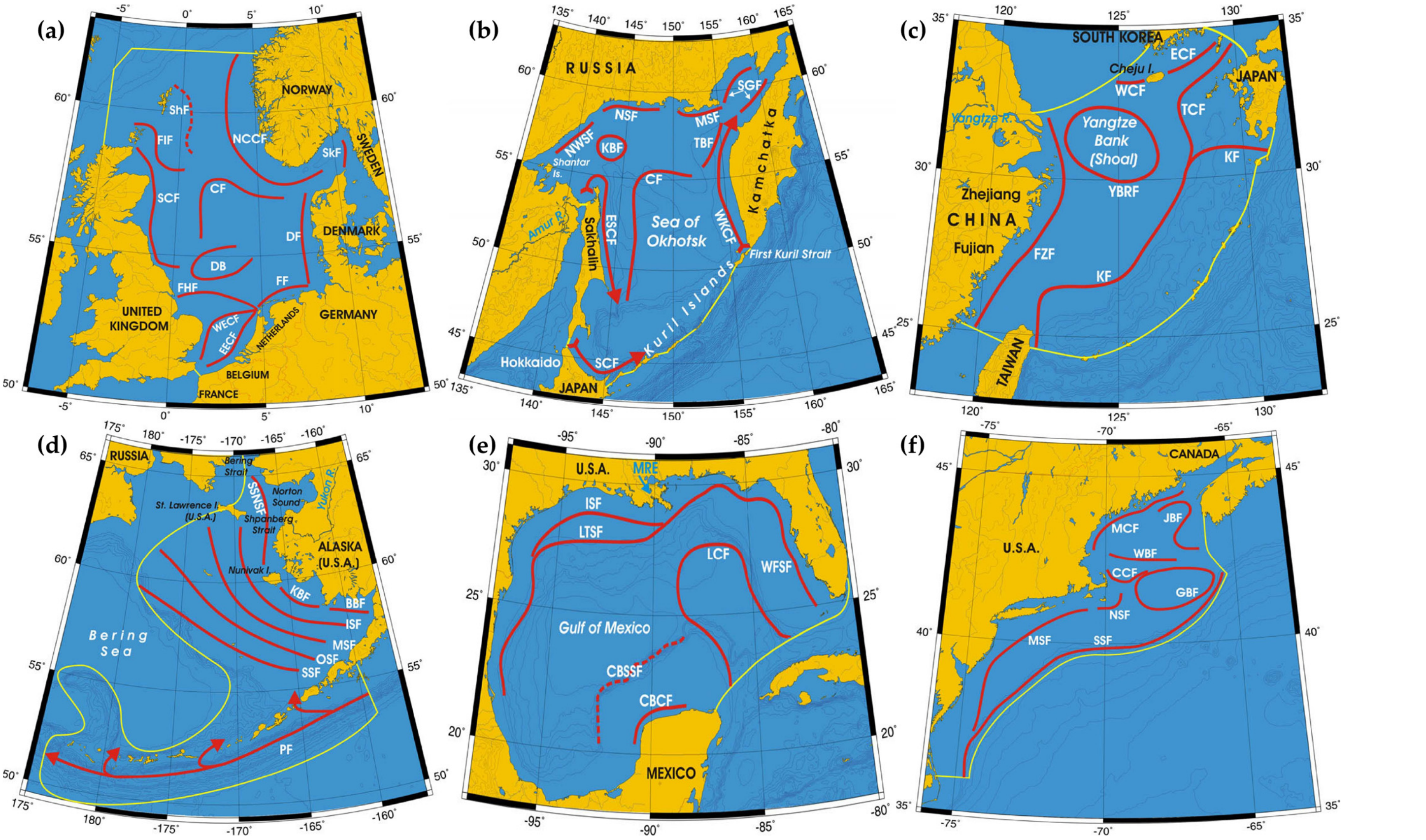

Figure 2. Distribution of main ocean fronts in some global sea areas [3]: (**a**) the North Sea; (**b**) the Sea of Okhotsk; (**c**) the East China Sea; (**d**) the East Bering Sea; (**e**) the Gulf of Mexico; and (**f**) the Northeast US Continental Shelf. The red lines represent the main axes of ocean fronts. The yellow lines represent the boundary of the Large Marine Ecosystems (LMF).

2.2.2. Artificial Intelligence Methods

Ocean fronts have been a subject of study for many years, and a variety of methods and algorithms have been proposed to address the problem of ocean fronts. However, all these existing ocean front recognition methods are built upon human expertise in defining the front based on subjective thresholds of relevant physical variables. In recent years, deep learning methods, especially convolutional neural networks (CNNs), have been applied to various remote sensing images processing tasks, such as cloud detection [39] and water body extraction [40]. With numerous learnable convolutional kernels, CNNs can extract rich features and use them to identify target objects from complex backgrounds. Therefore, deep learning is becoming an important part of several research-driven and operational geoscientific processing schemes, and functions as a provider of contextual cues for physical modeling [41]. A few researchers have begun to explore deep learning methods for extracting ocean fronts. Lima et al. [42] used an image classification network to determine whether a small patch from a grayscale SST image contained ocean fronts. Based on that, they later proposed a multi-scale deep framework (MDF) to better locate ocean fronts and reflect their strength [43] (Figure 3). To meet the need for visual interpretation and automatic ocean front detection in significant frontal areas, a novel method based on deep learning is proposed by Li et al. [44]. In this method, a deep learning model with U-Net architecture was designed to detect and locate significant frontal zones in grayscale SST images. The results showed that the proposed method could not only merge messy fronts but also capture the overall patterns of frontal zones and work with conventional methods to get a better frontal ridge extraction result. Li et al. [45] designed a bi-directional edge detection network (BEDNet) based on their collected ocean front data set. BEDNet mainly contains four stages, which can achieve bi-directional multi-scale information fusion. Moreover, they combined the dice and cross-entropy loss function to train the network, which obtained the fine-grained ocean front detection results. Lima et al. [46] proposed a deep learning approach for ocean front recognition that can automatically recognize the ocean front. It has fewer layers compared to existing architecture for the ocean front recognition task. In addition, they extended the proposed network to recognize and classify the ocean front into strong and weak ones. Due to the weak edge property of the ocean fronts, Li et al. [47] formulated ocean front detection as a weak edge identification problem and proposed the weak edge identification network (WEIN) for ocean front detection. The experimental results, in comparison to the traditional and deep learning approach, demonstrated the superiority of WEIN for ocean front detection. Xie et al. [48] proposed a semantic segmentation network called location and seasonality enhanced network (LSENet) for multi-class ocean fronts detection at the pixel level. This method could identify and distinguish various categories of ocean fronts with different behavior characteristics at different times and regions. Random forests are powerful classification and regression tools that are commonly applied in machine learning and image processing. Sun et al. [49] proposed cooperative profit random forests (CPRF). Experimental comparisons with several other existing random classification forest algorithms were carried out on several real-world data sets, and CPRF achieved promising results in ocean front recognition. Evolution Trend Recognition (ETR) was proposed by Yang et al. [50] to recognize the trend of ocean fronts. A novel classification algorithm was first proposed for recognizing the trend of ocean fronts. Then, the GoogLeNet Inception network was trained to classify the trend of ocean fronts. Experiment results showed that the proposed ETR algorithm was highly promising for trend classification of ocean fronts. Table 1 is a summary of the use of machine learning or depth learning to detect ocean fronts.

Table 1. Use of artificial intelligence methods to detect ocean fronts.

Researchers	Models/Methods	Effects/Objectives	Datasets/Resources
Lima et al. [42]	Convolutional neural networks (CNNs)	Determination of ocean fronts	National Oceanic and Atmospheric Administration (NOAA)
Lima et al. [43]	Multiscale deep framework (MDF)	Location and reflection of ocean fronts	Global satellite SST images
Li et al. [44]	A deep learning model with U-Net architecture	Better frontal ridge extraction of ocean fronts	Grayscale SST images
Li et al. [45]	Bi-directional edge detection network (BEDNet)	Fine-grained detection of ocean fronts	365 images based on the gradient of SST
Lima et al. [46]	Deep convolutional neural networks (deep CNNs)	Recognition and classification of ocean fronts	Remote sensing (RS) data
Li et al. [47]	Weak edge identification network (WEIN)	Better recognition of ocean fronts	365 RS images from satellite
Xie et al. [48]	Location and seasonality enhanced network (LSENet)	Pixel level detection of multi-class of ocean fronts	the Advanced Very High-Resolution Radiometer (AVHRR) SST daily data
Sun et al. [49]	Cooperative profit random forests (CPRF)	Better recognition of ocean fronts	Fourteen real-world datasets
Yang et al. [50]	Evolution trend recognition (ETR)	Recognition of the trend of ocean fronts	OFTreD and OFTraD

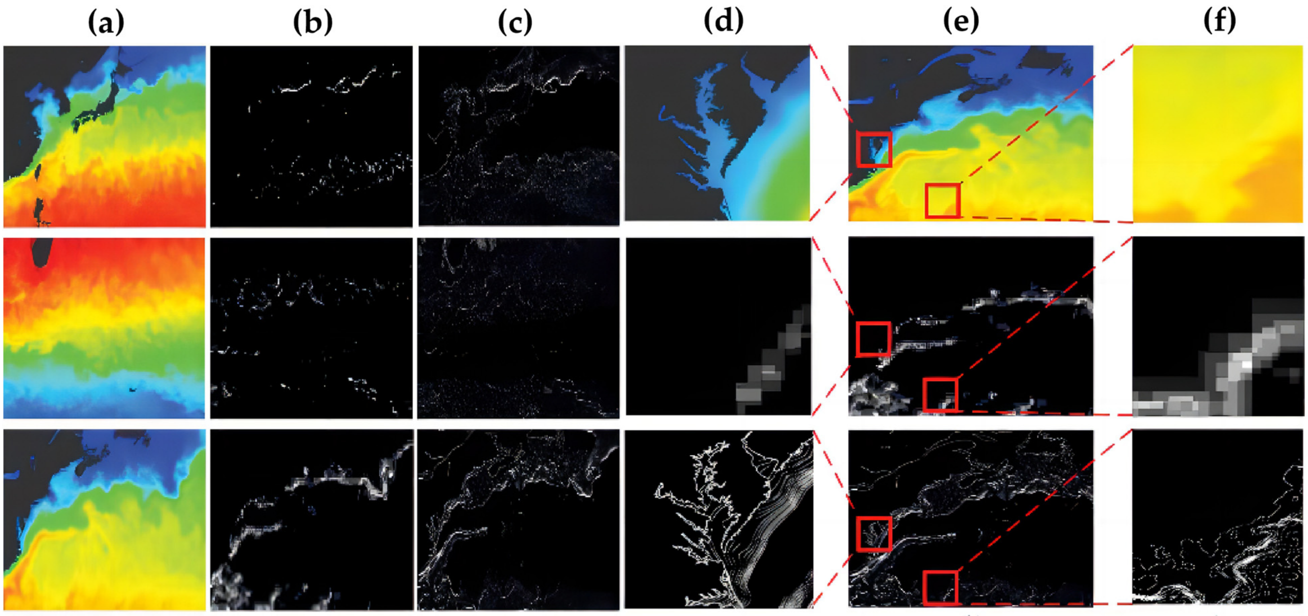

Figure 3. Comparison with the traditional method for ocean fronts detection [43]: (**a**) false color SST image; (**b**) multiscale deep framework (MDF); (**c**) traditional method; and (**d**)–(**f**) differences between MDF and the traditional method.

Compared with traditional oceanographic methods, these artificial intelligence methods based on machine learning or depth learning have played a unique advantage in the detection accuracy of the ocean front. With the further popularity of ocean big data, artificial intelligence methods will be more widely used and promoted. However, the shortcomings of their unclear physical meaning will gradually emerge, which is also a problem that needs to be solved in the future.

2.2.3. Detection Methods Based on SSP

When we pay more attention to the acoustic effects of ocean fronts, the SSP and its variation characteristics must become a research focus of underwater acoustics. It is a new method to detect the frontal zone by using cluster analysis of the SSP in recent years. Clustering analysis is a mathematical method to classify things or objects according to certain requirements, which uses a fuzzy mathematical language. The goal of cluster analysis is to collect data to classify based on similarity. The principle of cluster analysis is that the data in the same category have great similarities, and the data between different categories are very different. Due to the obvious differences in the structure of the SSP in the sea area where the ocean front exists, it is a reliable method to perform the category recognition of SSP to detect the ocean front by using cluster analysis of the SSP. The classification research of the SSP by cluster analysis was first used in the 21st century. Mandelberg et al. [51] used the hierarchical clustering method to classify the General Digital Environmental Model (GDEM) sound speed profiles of the North Atlantic and the Northeast Pacific. Wang et al. [52] used the World Ocean Atlas 2013 (WOA13) dataset, adopted the hierarchical clustering method to calculate the number of categories of the SSP in the Indian Ocean, conducted fuzzy c-means (FCM) clustering on the structure of the SSP in different seasons and typical SSP, and concluded that there were seven categories of sound speed distribution in the Indian Ocean. Abiva et al. [53] used principal component analysis (PCA) and self-organizing map (SOM) to automatically cluster the SSP. This method was applied to the maritime area of the Strait of Gibraltar to analyze the variation of the SSP over time and space to characterize the underwater environment. In addition, Dubberley and Zingerelli [54] applied fuzzy clustering to oceanographic parameters related to acoustics (mixed layer depth, SST, sound speed gradient, and so on), and divided them into multiple categories. The applicability of this method was proved by applying the parabolic model on World Ocean Database in 2005 (WOD2005) statistical sound speed profiles and fuzzy clustering categories. Meredith et al. [55] used the hierarchical clustering method to cluster the SSP obtained from the data in the Master Oceanographic Observation Data Set (MOODS), to reflect the temporal and spatial changes of the SSP. Liu and Chen [56] used PCA and SOM methods to cluster the 75–150 m sound speed profiles calculated by the Unstructured Grid Finite Volume Community Ocean Model (FVCOM) in the East China Sea region. The results showed that the regions corresponding to each category extend along the contour line, with the largest fluctuation in northern Taiwan. As far as the current research is concerned, many studies have applied cluster analysis and other related methods to the classification of sound speed profiles. As we pay more attention to the structural characteristics of the SSP in typical ocean environments, there are several studies on the clustering of the SSP under the mesoscale ocean phenomenon, such as the ocean front in specific sea areas. Chen et al. [20] used the K-means algorithm for the cluster analysis of sound speed profiles of the whole sea depth around the Kuroshio extension (KE), extracted three types of characteristic sound speed profiles, and established the Kuroshio extension front (KEF) sound speed characteristic model (Figure 4). Liu et al. [57,58] used the FCM algorithm to cluster the surface sound speed of the KE and determined the surface position of the frontal zone and its information. Considering the changing characteristics of the ocean front in different depth ranges, it is necessary to cluster sound speed profiles of the ocean front in different sea layers to reconstruct the geometric model of the ocean front, but there are few studies in this regard. Liu et al. [59] divided the set of sound speed profiles of the Luzon Strait (LS) into three layers and clustered the sound speed profiles of each layer to reconstruct the three-layer structure of the Kuroshio intrusion front (KIF). Although it is a layered reconstruction method for the ocean front, the number of layers is fixed at the beginning, that is, the layering principle is not fully considered, so the results are completely related to the initial value of layering, and there is no means to optimize the layering through iteration. Subsequently, they improved the method and proposed an ocean front reconstruction method based on the K-means algorithm iterative hierarchical clustering the SSP [60]. Compared with other existing methods, this method has the key step of iterative hierarchical clustering according to the accuracy of clustering results. The results of iterative hierarchical clustering of the SSP can reconstruct the ocean front. Using this method, they reconstructed the ocean front in the Gulf Stream-related Sea area and obtained the three-dimensional structure of the Gulf Stream front (GSF). The three-dimensional structure was divided into seven layers in the depth range of 0–1000 m. According to our report, we summarized the relevant research and results in this area and produced Table 2 to obtain a more intuitive display.

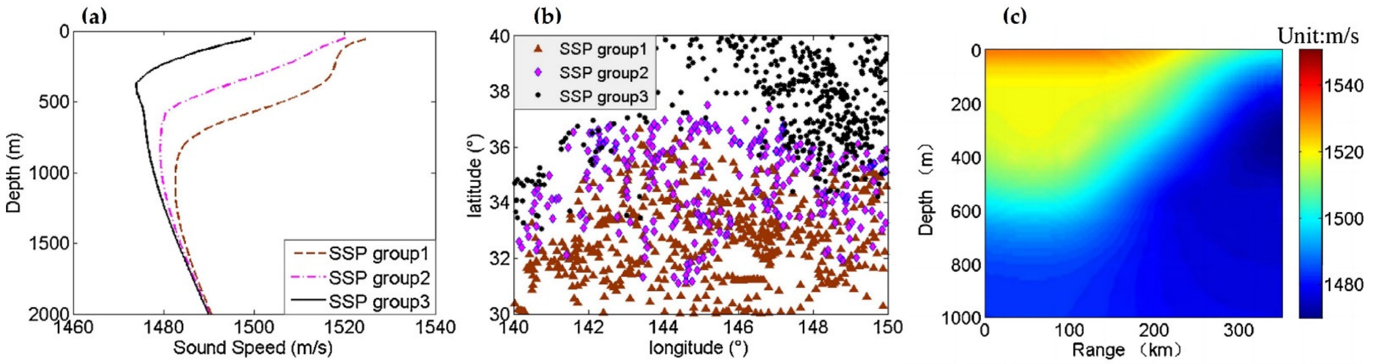

Figure 4. Results of cluster analysis and the KEF sound speed characteristic model [20]: (**a**) major feature of the three kinds of SSP; (**b**) spatial distributions of the three SSP groups; and (**c**) the KEF sound speed characteristic model.

Table 2. Application of clustering methods in the ocean environment and sound speed profiles.

Researchers	Methods	Research Object	Data Source
Mandelberg et al. [51]	The hierarchical clustering method	The SSP of the North Atlantic and the Northeast Pacific	GDEM
Wang et al. [52]	FCM	The SSP in the Indian Ocean	WOA13
Abiva et al. [53]	PCA and FOM	The SSP of the Strait of Gibraltar	Observation data
Dubberley and Zingerelli [54]	Fuzzy clustering	Oceanographic parameters	WOD2005
Meredith et al. [55]	The hierarchical clustering method	The SSP	MOODS
Liu and Chen [56]	PCA and SOM	The SSP in the East China Sea	FVCOM
Chen et al. [20]	The K-means algorithm	The SSP of the KE	Argo WOA09
Liu et al. [57,58]	FCM	The SSP of the KE	HYCOM
Liu et al. [59]	FCM and other methods	The SSP of the LS	HYCOM
Liu et al. [60]	FCM	The SSP of the Gulf Stream-related Sea	HYCOM

It is worth noting that the identification of the SSP through clustering analysis to detect ocean fronts is the most direct and crucial for studying the acoustic effects of ocean fronts. Therefore, this method should be popularized in future research on ocean front acoustic effects.

3. Theoretical Modeling of the Ocean Front

Ocean front feature modeling is a method to obtain the fine two-dimensional or three-dimensional structure features of the ocean front quickly and effectively. This is based on the mathematical model of ocean front spatial geometric structure by using remote sensing data, limited observation data, and historical data, combined with the typical structural features of ocean front that have been statistically analyzed at present. Based on the theme of our report, we divide the theoretical modeling of the ocean front into two parts: traditional oceanographic modeling, and sound speed field modeling for acoustic effect research.

3.1. Oceanographic Modeling

Oceanographic modeling here refers to the two-dimensional or three-dimensional parameterized description of ocean fronts of different types and regions through conventional oceanographic parameters, such as temperature, salinity, and velocity, to show the outstanding characteristics of ocean fronts. Oceanographers have done a lot of valuable work over the past decades, which is also helpful to the current research on ocean front modeling. Gangopadhyay et al. [61] reported feature-oriented regional modeling of ocean fronts. The large-scale meandering frontal systems such as the Gulf Stream, Kuroshio, and Brazil current, can be represented by speed-based feature models. Buoyancy forced coastal water mass fronts, such as the coastal currents, tidal fronts, plume fronts, dense ocean fronts, and inflow/outflow fronts, can be represented by a generalized parameterized water mass feature model. The interface region of the deep ocean and the coastal region can be modeled by a melding of two water masses along and across a prescribed isobath in the form of a shelf-break front. Table 3 shows the feature model classification of ocean fronts in the world's oceans according to [61]. The application of this modeling methodology for the rapid assessment of any regional ocean, based on limited data and resources, is now possible. The parameterized description was carried out for different types of ocean fronts in the Gulf of Maine and Georges Bank (GOMGB) region [62], mainly including the buoyancy-driven Maine Coastal Current (MCC), the shelf-slope front (SSF), the Georges Bank anticyclonic frontal circulation system, including the tidal mixing front (TMF), the basinscale cyclonic gyres, the deep inflow through the Northeast Channel (NEC), and the shallow outflow via the Great South Channel (GSC). Carrière [63] developed feature models as parameterization schemes for the range-dependent temperature field when the latter is mainly influenced by thermal fronts. The proposed feature-model parameterization is shown to provide robust estimates of the two-dimensional temperature field even when the simulated environment presents smaller scale inhomogeneities.

Table 3. The feature model classification of ocean fronts in the world's oceans [61]. ECSCC: East China Sea Coastal Current; SCSCC: South China Sea Coastal Current; NEC: North Equatorial Current; NECC: North Equatorial Counter Current; SEC: South Equatorial Current; SECC: South Equatorial Counter Current.

Region	**Deep (Boundary Currents, Meanders, and Jets)**	**Coastal (Water Mass Fronts, Upwelling Fronts, Transition Regions, Tidal Fronts)**
Western North Atlantic	Gulf Stream, deep western boundary current	Maine coastal current, Georges Bank tidal fronts, shelf-slope front
Eastern North Atlantic	Azores current, Canary current, Portugal current	Upwelling fronts in northwest Africa
Western Pacific	Kuroshio, deep western boundary current	Yellow Sea coastal current, Korean coastal current, ECSCC, SCSCC, Taiwan warm current, Tsushima current
North Pacific	North Pacific current, California current system	Alaskan coastal current, Alaskan stream, Prince William sound circulation system
South Pacific	East Australian current, Humbolt current	Upwelling fronts in central Chile
Northwest European shelf and the Bering Sea	Labrador current, north Atlantic current	Norwegian current, tidal mixing fronts, Celtic Sea shelf-break front
Equatorial Pacific	Equatorial current systems	Upwelling fronts, NEC, NECC, SEC, SECC
Southern Ocean	Antarctic circumpolar current	Agulhas retroflection current, Weddell front, Antarctic circumpolar shelf front
Indian Ocean	Somali current, Agulhas current, Western India undercurrent	North Indian coastal current, east African coastal current

Ocean front feature modeling is very useful as a means of compressing grid data. It can transmit data to ships at sea and assimilate data into ocean models [64]. For assimilation, feature modeling is helpful to link the easily obtained satellite remote sensing surface data with the less common field measurement data to simulate the ocean front structure in a way of maintaining the oceanographic feature structure.

3.2. Sound Speed Field Modeling for Acoustic Effect Research

Sound speed in seawater is a function of temperature, salinity, and pressure (depth). Although we can obtain the sound speed distribution of the ocean front according to the parameterized model of the ocean front in the previous section through the empirical formula [65], it is more important to use fewer sound speed profiles to obtain the two-dimensional or three-dimensional sound speed distribution of the ocean front directly, when we only have the observation data of sound speed. This step is also the core and basis of studying the acoustic effects of ocean fronts. Based on observational data, a parametric model of shallow (less than 300 m) deep-ocean fronts was constructed via sound speed profiles which were trilinear with depth by Rousseau et al. [66]. The model was sufficiently general to permit the determination of acoustical effects for fronts of varying strengths, vertical extents, and positions within the propagation range. They introduced a parametric model including the location and orientation of a shallow-water front, as well as jumps in sound speed and current across it [67]. A corresponding system of equations might be inverted so that travel-time changes could be used to predict estimates for frontal geometry, sound speed, and current discontinuities across an ocean front. To research the behavior of sound near an ocean front in a region with wedge bathymetry, the front was parameterized as a zone of variation with inshore and offshore boundaries parallel to a straight coastline [68]. By analyzing Argo data and the sea surface height (SSH) data in this Kuroshio Extension area, a two-dimensional sound-speed feature model (SSPFM) characterizing the KEF is proposed by Chen et al. [20]. With reanalysis data from the hybrid coordinate ocean model, a three-dimensional sound-speed environment of the KEF is established, which establishes the foundation for the following acoustic effect research. According to the two-dimensional parameterized model of the ocean temperature front constructed by Carriere [63], Liu et al. [69] built a two-dimensional parameterized feature model of the ocean front based on the SSP (Figure 5), calculated, and compared the influence of the ocean front on convergence area by setting different ocean front environment.

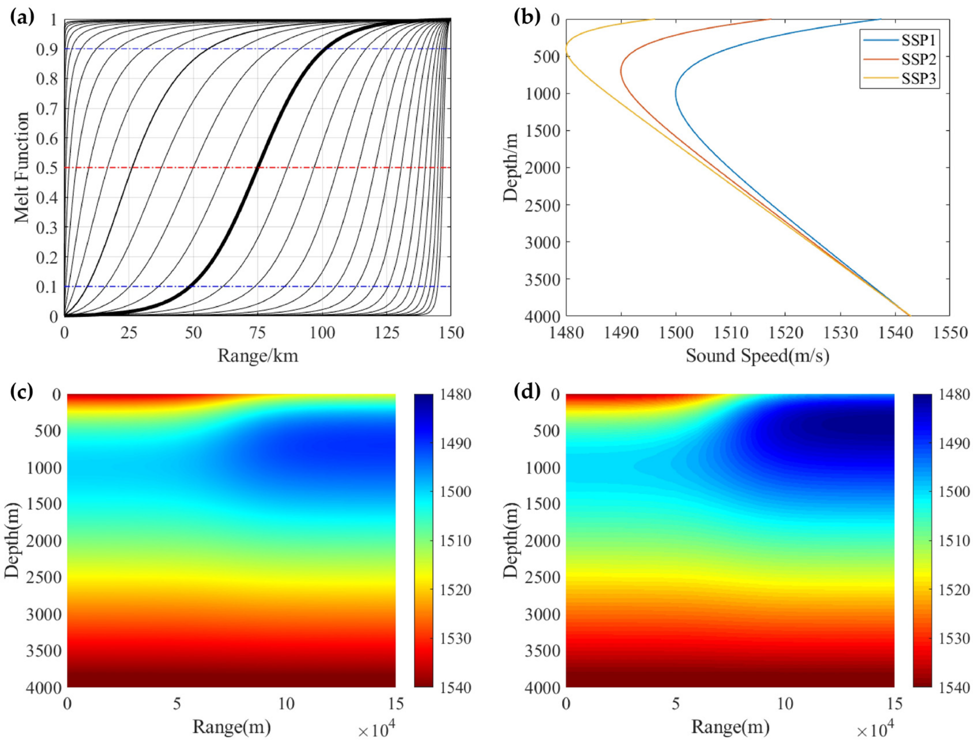

Figure 5. Ocean front model based on SSP [69]: (**a**) the variation of melt function with the range in ocean front model. The blue lines show the melt function at 0.1 and 0.9, respectively, while the red line represents the melt function at 0.5; (**b**) three typical sound speed profiles as input of ocean front model; and (**c**,**d**) the distribution of sound speed field of ocean front with different intensity output from the model.

The direct significance of the parameterized sound speed field in the ocean front area is that it can intuitively understand the sound speed distribution of the ocean front, to better research the acoustic effects of the ocean front. In addition, compared with the traditional acquisition method, the direct construction of the ocean front sound speed field can reduce the error brought by the calculation of the SSP in the temperature-salt profile.

4. Acoustic Effects of Ocean Fronts

The ocean front will affect the sound propagation effect in the sea area, which will have an important influence on the detection performance of the sonar system. For the study of acoustic effects of ocean front, one method is simulation analysis, that is, the effect of ocean front on acoustic propagation is described qualitatively or quantitatively by ocean front parametric model and specific sound field calculation program (this method does not rely on the actual acoustic experimental data in the study area, which is of general significance). Another is to conduct field acoustic experiments in the sea area where the ocean front exists to study the acoustic effects and rules of a specific ocean front.

4.1. Analysis of the Simulation

The existence of the ocean front changes the original horizontal or vertical uniform environment, which makes the distribution of sound speed field present an uneven feature. In this case, the sound rays emitted from the sound source will show different bending, refraction, and reflection from the normal environment with the increase of the propagation distance, which will eventually have a significant impact on the reception of the sonar system. Rousseau et al. [66] used ray theory to investigate the effects of sound-speed variations produced by shallow (less than 300 m) deep-ocean fronts on short-range acoustic transmission between surfaced sound source and receiver. Frontal influences on travel time and geometrical spreading loss are examined, and expressions for per-ray amplitude and phase are developed for CW transmissions with source and receiver near the surface. All frontal quantities are demonstrated to produce significant acoustical variations, such as total field transmission loss (TL) change of more than 6 dB. Heathershaw et al. [12] used three-dimensional numerical ocean model data as input and calculated the acoustic effects of relevant mesoscale phenomena. The results showed that for different sound sources and receiving depths, the effects of the front and eddy increase the TL by 10–20 dB, which was comparable with the magnitude of the frontal effect that was seen in studies using analytical models of ocean fronts and with acoustic calculations. From a perspective of sound propagation, a sloping bottom found in typical shallow-water environments can cause propagating sound to horizontally refract offshore. Additionally, an offshore ocean front can cause horizontal reflection/refraction shoreward. Combining these two effects, Lin et al. [10] believed sound tends to propagate along the front, and "whispering gallery" modes can be observed. The whispering gallery means that sound waves can continuously reflect between the ocean front and the coast with little TL, so sound can travel a long distance along the ocean front. They modeled this effect via a three-dimensional acoustic propagation program exploited in the Acoustics Toolbox (AT, https://oalib-acoustics.org/models-and-software/acoustics-toolbox/ (accessed on 1 July 2021)). The results showed sound energy trapped ahead of the front with observable frequency and modal dependence. Additionally, when including the foot of the front, which was commonly seen on the continental shelf and extended inshore along the bottom, the model showed less modal attenuation, which raised the level of the trapped energy. Based on the above research, they discussed the consequence of this whispering gallery effect on array processing [70]. Specifically, the influence of an ideal ocean front on the array gains was studied. Since the sound reflecting from the ocean front forms highly correlated beams, the array gain of a horizontal hydrophone array would be increased. Computer simulations (including the Oyashio and the Kuroshio fronts and the eddy model such as a Gulf Stream ring) were used by Weinberg et al. [71] to investigate horizontal acoustic refraction through strong ocean fronts and solitary mesoscale eddies. Using purely horizontal refraction, ignoring other effects, horizontal deflections more than 1° were computed. Mellberg et al. [72] used numerical experiments, including the germinating ray acoustic simulation system (GRASS) model and the wide-angle finite-difference PE model (IFD/PE) of Lee and Botseas, to present the environmental acoustic effects of the western Greenland Sea Frontal Zone in the summer of 1983 along a 185 km west-to-east transect. The front can impart >15 dB increases in TL in <10 km. They also discussed the effects of the frontal zone on sound propagation as a function of the location and depth of the acoustic source and the depth of the receiver, sometimes the TL could be greater than 20 dB. Jin et al. [7] considered normal mode coupling due to a shallow water coastal front and used oceanographic data from the 1992 Barents Sea Polar Front (BSPF) experiment as input to normal mode and parabolic equation (PE) acoustic propagation models. Criteria for the sensitivity of mode coupling to coastal front widths were derived and applied to the BSPF as a representative example. Shapiro and Thain [73] studied patterns and seasonal variations of underwater noise in the Celtic Sea by using a coupled ocean model (POLCOMS) and an acoustic model (HARCAM) in the year 2010. The results showed that when the sound source was on the onshore side of the front, the sound energy was mostly concentrated in the near-bottom layer in summer.

While in winter, the sound from the same source was distributed more evenly vertically. When the sound source was on the seaward side of the front, the sound level was nearly uniform in the vertical. Figure 6 shows some research results according to [73]. Based on the parameterized model, the influence of the ocean front on the location of the convergence zone was studied [69]. The results showed that when the sound wave propagated from the warm water mass to the cold water mass, the convergence area moved forward, and the degree of the forward movement changed with the intensity of the ocean front; when the propagation direction was opposite, the convergence area moved backward. In addition, they applied the melt function to forecast the depth of the convergence area in the ocean front environment through the parameterized model [58] (Figure 7). The root mean square error (RMSE) between the forecasting result and the actual calculation result through the ray model in the second detection convergence area was 43.3 m, and the forecasting effect was better, which could provide good guidance for the acoustic concealment of the target under the environment of ocean front.

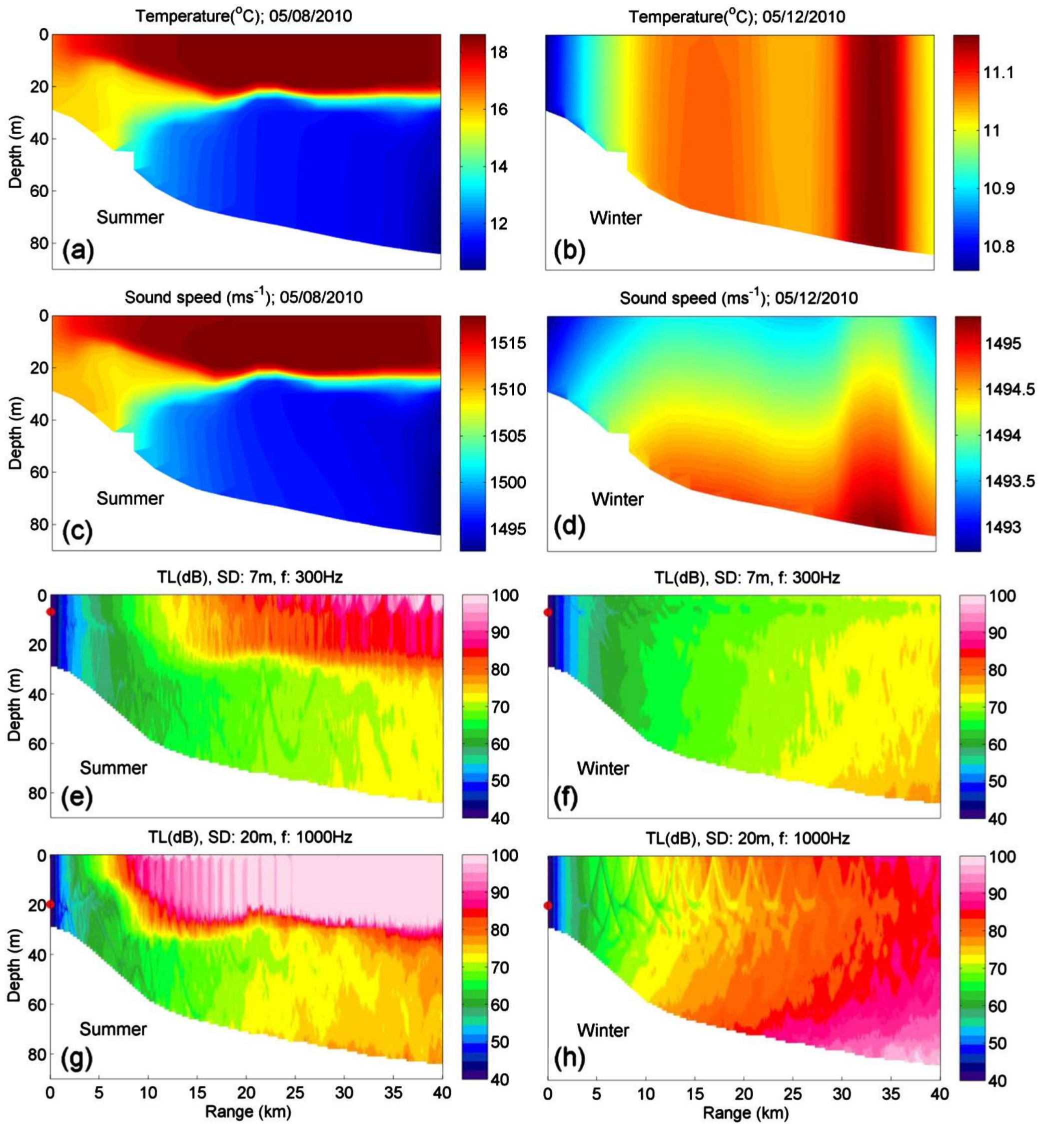

Figure 6. Seasonal variations of parameters when the sound source was on the onshore side of the ocean front in the Celtic Sea [73]: (**a**,**b**) temperature distribution; (**c**,**d**) sound speed distribution; (**e**,**f**) the TL at frequency 300 Hz with source depth 7 m; and (**g**,**h**) the TL at frequency 1000 Hz with source depth 20 m. The position of red dots represents the depth of the sound source.

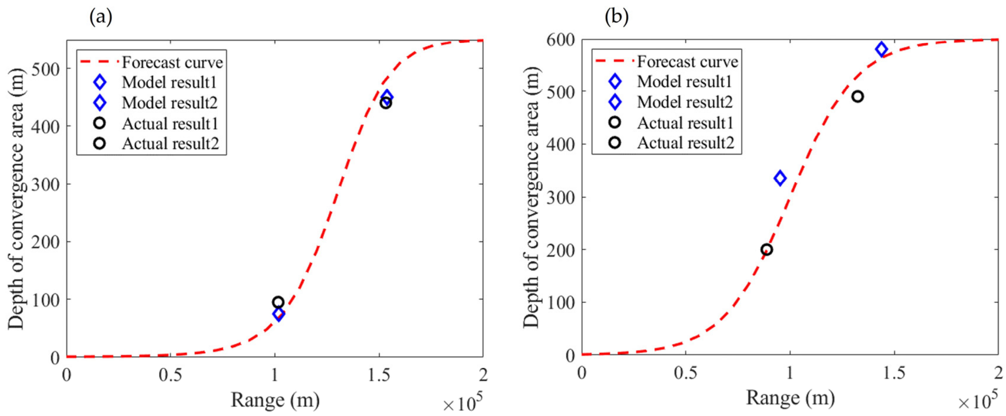

Figure 7. The forecasting curve of the depth of the convergence area (the red dotted line) and the calculating results of the model (blue dots) and actual ocean front (black dots): (**a**) 1 January, representing winter; (**b**) 1 July, representing summer. The forecasting results using the melt function were in good agreement with the model and the actual results, which proved that the melt function was applied to effectively achieve the depth forecast of the convergence area in the ocean front environment.

4.2. Experimental Study

In recent years, with the enhancement of ocean observation capability and the rapid development of various underwater acoustic instruments, research on the acoustic effects of ocean fronts has been greatly promoted, especially the valuable data obtained from acoustic experiments. This will help us better understand the characteristics and laws of sound propagation in various specific ocean environments. Lynch et al. [74] used the high-resolution data from the 1996–1997 New England shelf break experiment to examine the spatial and temporal variability of the acoustic field in the region of a strong coastal shelf break front. Several interesting propagation effects were noted; the most interesting was the inhibition of strong acoustic-bottom interaction by the warm shelf water beneath the shelf break front, and the existence of small-scale ducts near the front, due to offshore transport. Ramp et al. [75] used the data of the Asian Seas International Acoustics Experiment (ASIAEX) in 2001 and found that, as a result of the Kuroshio front, the sound rays refracted downward. After passing through the shelf break front, the sound signal attenuated rapidly. They considered the influence of the uncertainty of the marine environment on the sonar operating distance from the perspective of sound ray propagation. Using a 93 Hz signal, the Lloyd mirror effect was found by Moore et al. [76] when the sound source depth was 50 m, and the sound ray was at a small grazing angle. This is because the presence of the front makes the incident sound wave generate total internal reflection. The direct and reflected modal rays can constructively interfere, having the potential to increase the intensity level by 6 dB. Deferrari [77] examined sound propagation for both environments with data from two similar fixed system propagation experiments: one for the prograde front environment of the coast of south Florida near the site of the Acoustic Observatory; and the second for the retrograde front environment of the Mid-Atlantic Bight. He observed intensity fluctuations and temporal coherencies of broadband acoustic signals over several octaves to vary with variations of the sound speed. Liu et al. [11] introduced a joint experiment of ocean acoustic and physical oceanography at the Western North Pacific fronts. The measurement data for sound waves passed through the ocean front was processed. It was found that the TL presented some difference when the source was in the front center and sound waves propagated towards water mass on opposite sides of the front center (Figure 8). Moore et al. [78] presented acoustic data collected on two Webb Slocum gliders during the Shallow Water Experiment (SW06) on the continental shelf off New Jersey. A major goal of these measurements was to quantify the three-dimensional propagation effects of the ocean front. Jensen et al. [79] calculated propagation through a real front observed on the Iceland-Faroe Ridge through the oceanographic data (conductivity, temperature, depth (CTD) sensors, expendable bathythermograph (XBT), thermistor chain) in the frontal area. They found that the acoustic effects of the front were significant (>10 dB), but with a strong dependence on environmental parameters as well as on source/receiver depth and frequency. Kravchun [80] described the hydrographic characteristics of the benthic front with the use of data from the international WOCE experiment. Meanwhile, he estimated the changes introduced by the benthic front into the phase and group velocities and the vertical structure of modes. In the summer of 1996, an integrated acoustic-oceanographic experiment was carried out in the Middle Atlantic Bight to study the dynamics of the shelf break front and the effects of frontal variability on sound propagation. Chiu et al. [81] reported the results of an acoustic tomographic analysis of frontal variability.

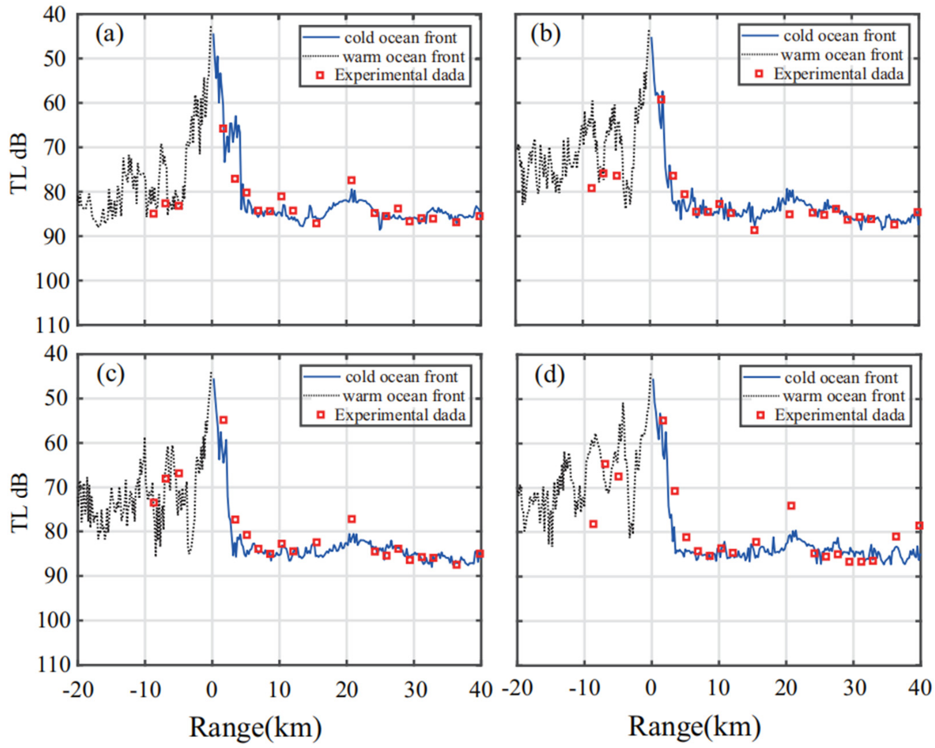

Figure 8. The TL in cold side (blue dotted line), warm side (black line), and experimental results with 100 m explosions (red square) in depths of: (**a**) 75 m; (**b**)150 m; (**c**) 175 m; and (**d**) 200 m [11].

With the development of more and more marine acoustic experiments, these valuable experimental data will help us better understand the characteristics and laws of sound propagation in various specific marine environments.

5. Conclusions

In this paper, we review the research progress of ocean fronts and their acoustic effects. The whole research process is summarized, and the technical route is given in Figure 9. Different from previous studies, we pay more attention to the acoustic perspective. The definition of ocean fronts, detection methods, modeling research, and the theoretical and experimental research of acoustic effects are reported in turn, which is easier for readers to understand.

As a narrow transition zone between two or more water masses with obviously different properties, the detection method based on an oceanographic perspective has a clearer physical meaning, but the threshold value of a such method is often difficult to determine, such as the gradient method. In recent years, with the rapid development of artificial intelligence, many detection methods are based on machine learning or deep learning and have achieved good results. However, it should also be noted that machine learning methods rely on large data sets. When this condition cannot be met, it may not be effective. Because we pay more attention to the acoustic effect of the ocean front, the detection method based on the SSP has also been reported in this paper. This method is more direct and effective and can establish a direct connection with the acoustic effect of the ocean front.

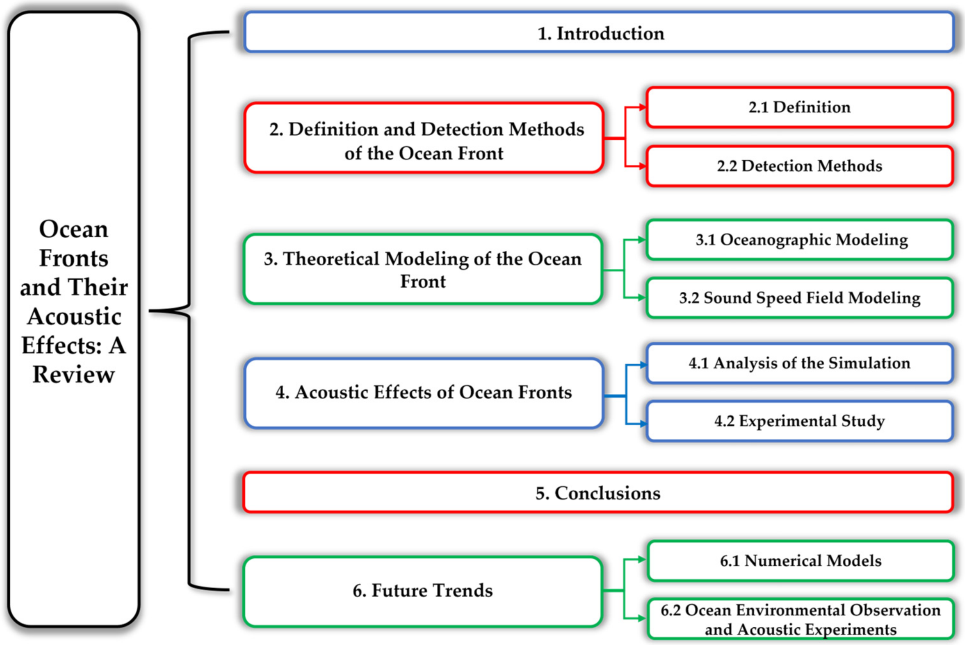

Figure 9. The technical route of the research process.

Based on the theme of the report, we divide the theoretical modeling of the ocean front into two parts: traditional oceanographic modeling, and sound speed field modeling for acoustic effect research. With the deepening of oceanographers' research on ocean phenomena at various scales, their theoretical model research has reached a new height. These parameterized models have universal significance for studying the characteristics of ocean fronts and their acoustic effects. At present, research on the parameterization modeling of the ocean front is still in the simulation stage. How to consider the combination of modeling research and actual ocean front environment to achieve more accurate results is a problem that needs to be focused on.

The ocean front will affect the sound propagation effect in the sea area, which will have an important influence on the detection performance of the sonar system. For the study of acoustic effects of the ocean front, one method is simulation analysis. In the reality of limited experimental conditions and insufficient measured data, it is particularly important to study the theoretical model of the ocean front and its acoustic effects. Another method is to conduct field acoustic experiments in the sea area where the ocean front exists to study the acoustic effects and rules of a specific ocean front. These valuable experimental data help us better understand the characteristics and laws of sound propagation of ocean fronts.

6. Future Trends

6.1. Develop High Resolution and Accuracy Numerical Models

The ocean numerical model is a numerical model that can quantitatively describe ocean phenomena and their changes. It reflects complex processes such as ocean dynamics, physics, and their interactions by establishing mathematical and physical equations. It discretizes the continuous ocean fluid movement, and the earth's space is divided into three-dimensional grid structures in longitude, latitude, and vertical directions, and then the partial differential equations are solved by numerical integration [82]. With the deepening of our understanding of the oceans and the rapid development of computer technology, the development and application of global ocean models have become one of the important directions of geoscience research. The ocean model can not only be used in the research of ocean science itself, but also widely used in the simulation and prediction research of climate and environmental change and provide technical support for the development of marine resources, national defense security, and other major national needs. With the continuous deepening of the ocean and climate change research, ocean numerical models are gradually developing towards higher resolution (the higher the resolution, the finer the grid), more physical processes (the increase in the number of equations), and faster computing speed [83]. At present, the number and types of ocean observation data are increasing, and the computing speed of high-performance computers is moving from the "P" level (PetaFlops) to the "E" level (ExaFlops) [84]. Artificial intelligence, especially deep learning, has developed rapidly [85], which provides opportunities for the rapid development of high-resolution and accurate ocean numerical models, and poses new challenges.

The three-dimensional ocean circulation model is the core of the ocean system. For such ocean dynamic phenomena as mesoscale eddies and fronts, the model resolution is an important factor. Only when the horizontal resolution of the model is less than or equal to the local first baroclinic Rossby deformation radius, the model can distinguish mesoscale eddies and fronts. Such a model is called the vortex identification model [86]. Taking offshore China as an example, the China offshore regional operational forecast system of the National Marine Environmental Forecasting Center has been equipped with the resolution for the identification of the part of ocean fronts. In the future, more detailed regional models will be developed in the local sea area, which can simulate some secondary mesoscale eddies and fronts with smaller spatial scales. For large cross-latitude sea areas, the difference in Rossby deformation radius is huge, and the seasonal variation of stratification is large, which has a greater impact on the baroclinic Rossby deformation radius. Therefore, the setting of model resolution should be considered in the development of the fine region model.

6.2. Conduct Extensive Ocean Environmental Observation and Acoustic Experiments

The accurate study of acoustic effects of ocean fronts and various typical oceanic phenomena requires actual ocean hydrological observation data and field acoustic experiment data. At present, we can obtain long-term observation data mainly through buoy observation technology, submersible buoy observation technology, and seabed observation technology. In addition, we can also get real-time environmental data of a certain region through CTD, XBT, Acoustic Doppler Current Profilers (ADCP), and so on. In the future, we need to conduct more extensive ocean environmental observations to meet the needs for studying ocean acoustics.

The development of marine acoustics cannot be separated from acoustic experiments. Many experimental studies on sound propagation in dynamic marine environments have been carried out worldwide. Shallow sea acoustic experiments mainly include the Barents Sea Polar Front (BSPF) sound propagation experiment in 1992 [87], the SWARM internal wave acoustic scattering experiment in 1995 [88], the ASIAEX South China Sea experiment in 2001 [89], the Yellow Sea acoustic experiment in 2005 [90], the shallow water experiment in 2006 (SW06) [91], and so on. Deep sea acoustic experiments mainly include the Northeast Pacific experiment (SLICE89) [92], the North Pacific Acoustic Laboratory experiment (NPAL) [93], the Acoustic Engineering Test (AET) in 1994 [94], theATOC95 experiment [95], the long-range ocean acoustic propagation experiment (LOAPEX) [96], and so on, which are carried out by the United States in the North Pacific Ocean and are collectively referred to as NPAL experiments. In addition, the PhilSea experiment carried out in the Philippines Sea in the Northwest Pacific from 2009 to 2011 is the first large-scale comprehensive acoustic experiment carried out in the complex deep-sea area [97]. These acoustic experiments have greatly promoted our understanding of the marine environment and its acoustic effects and provided a great reference for the further development of this field in the future. We need to further promote the relevant experiments of ocean acoustics to accelerate research on the acoustic effects of the ocean environment.

The future trends in this field are multifaceted. On the premise of the increasingly mature theory of ocean acoustics, it is undeniable that enriching ocean hydrological data, including satellite observation data, numerical model data, marine survey data, and acoustic experiment data, will further promote the understanding of typical marine environments such as ocean fronts and their acoustic effects. Of course, we cannot do without some new AI methods mentioned previously in the process. We can not only apply AI methods to the detection of ocean fronts but also acoustic tomography. The new methods in the future will further provide more help for the study of ocean fronts and their acoustic effects.

Author Contributions: Conceptualization, W.C. (Wei Chen) and Y.L. (Yuyao Liu); methodology, Y.L. (Yuyao Liu) and W.C. (Wen Chen); formal analysis, Y.C. and Z.M.; investigation, W.C. (Wen Chen) and Y.L. (Yuyao Liu).; resources, Y.L. (Yuyao Liu), Y.L. (Yan Liang) and Y.C.; writing—original draft preparation, Y.L. (Yuyao Liu) and W.C. (Wei Chen); writing—review and editing, W.C. (Wei Chen) and Z.M. All authors have read and agreed to the published version of the manuscript.

Funding: This research received no external funding.

Institutional Review Board Statement: Not applicable.

Informed Consent Statement: Not applicable.

Data Availability Statement: Not applicable.

Conflicts of Interest: The authors declare no conflict of interest.

References

1. Khan, S.; Song, Y.; Huang, J.; Piao, S. Analysis of underwater acoustic propagation under the influence of mesoscale ocean vortices. *J. Mar. Sci. Eng.* **2021**, *9*, 799. [CrossRef]
2. Levine, M.D. Internal waves in the ocean: A review. *Rev. Geophys.* **1983**, *21*, 1206–1216. [CrossRef]
3. Belkin, I.M.; Cornillon, P.C.; Sherman, K.E. Fronts in large marine ecosystems. *Prog. Oceanogr.* **2009**, *81*, 223–236. [CrossRef]
4. Cao, L.; Tang, R.; Huang, W.; Wang, Y. Seasonal variability and dynamics of coastal sea surface temperature fronts in the East China Sea. *Ocean Dyn.* **2021**, *71*, 237–249. [CrossRef]
5. Chen, H.; Qi, Y.; Wang, Y.; Chai, F. Seasonal variability of SST fronts and winds on the southeastern continental shelf of Brazil. *Ocean Dyn.* **2019**, *69*, 1387–1399. [CrossRef]
6. Mooers, C.N. Oceanic fronts and their effects on underwater acoustics. *J. Acoust. Soc. Am.* **1978**, *63*, S87. [CrossRef]
7. Jin, G.; Lynch, J.F.; Chiu, C.; Miller, J.H. A theoretical and simulation study of acoustic normal mode coupling effects due to the Barents Sea Polar Front, with applications to acoustic tomography and matched-field processing. *J. Acoust. Soc. Am.* **1996**, *100*, 193–205. [CrossRef]
8. Lohmann, R.; Belkin, I.M. Organic pollutants and ocean fronts across the Atlantic Ocean: A review. *Prog. Oceanogr.* **2014**, *128*, 172–184. [CrossRef]
9. Xue, R.; Yang, Y.; Weng, J.; Wen, H.; Chen, H.; Lin, L. Modelling convergence zone propagation under the influence of Arctic Front. In Proceedings of the 2021 OES China Ocean Acoustics (COA), Harbin, China, 14–17 July 2021; pp. 229–233. [CrossRef]
10. Lin, Y.; Newhall, A.E.; Lynch, J.F. The effect of an ocean front on sound propagation in shallow water. *J. Acoust. Soc. Am.* **2006**, *120*, 3182. [CrossRef]
11. Liu, J.; Piao, S.; Zhang, M.; Zhang, S.; Guo, J.; Gong, L. Characteristics of three-dimensional sound propagation in Western North Pacific fronts. *J. Mar. Sci. Eng.* **2021**, *9*, 1035. [CrossRef]
12. Heathershaw, A.D.; Stretch, C.E.; Maskell, S.J. Coupled ocean-acoustic model studies of sound propagation through a front. *J. Acoust. Soc. Am.* **1991**, *89*, 145–155. [CrossRef]
13. Chen, C.; Lei, B.; Ma, Y.; Liu, Y.; Wang, Y. Diurnal fluctuation of shallow-water acoustic propagation in the cold dome off northeastern Taiwan in spring. *IEEE J. Ocean. Eng.* **2020**, *45*, 1099–1111. [CrossRef]
14. Bost, C.A.; Cotté, C.; Bailleul, F.; Cherel, Y.; Charrassin, J.B.; Guinet, C. The importance of oceanographic fronts to marine birds and mammals of the southern oceans. *J. Mar. Syst.* **2009**, *78*, 363–376. [CrossRef]
15. Belkin, I.M. Front. In *Interdisciplinary Encyclopedia of Marine Sciences*; Nybakken, J.W., Broenkow, W.W., Vallier, T.L., Eds.; Grolier: Danbury, CT, USA, 2002; pp. 433–436.
16. Wu, S.; Li, Z.; Qin, J.; Wang, M.; Li, W. The effects of sound speed profile to the convergence zone in deep water. *J. Mar. Sci. Eng.* **2022**, *10*, 424. [CrossRef]

17. Huang, J.; Luo, Y.; Li, Y.; Shi, J.; Zheng, X.; Wang, J. Analysis of sound speed profile in the South China Sea based on empirical orthogonal function algorithm. In Proceedings of the 2021 OES China Ocean Acoustics (COA), Harbin, China, 14–17 July 2021; pp. 229–233. [CrossRef]
18. Kiryanov, A.V.; Salnikov, B.A.; Salnikova, E.N.; Slesarev, N.Y. Regional variability of influence of small-scale sound-speed fluctuation levels on the acoustic field's formation in the ocean. *IOP Conf. Ser. Earth Environ. Sci.* **2019**, *272*, 022144. [CrossRef]
19. Xu, W.; Schmidt, H.R. System-orthogonal functions for sound speed profile perturbation. *IEEE J. Ocean. Eng.* **2006**, *31*, 156–169. [CrossRef]
20. Chen, C.; Yang, K.; Duan, R.; Ma, Y. Acoustic propagation analysis with a sound speed feature model in the front area of Kuroshio Extension. *Appl. Ocean Res.* **2017**, *68*, 1–10. [CrossRef]
21. Zhang, Y.; Yang, K.; Xue, R.; Huang, C.; Chen, C. Convergence zone analysis for a source in the front area of Kuroshio Extension based on Argo data. In Proceedings of the OCEANS 2019–Marseille, Marseille, France, 17–20 June 2019; pp. 1–4. [CrossRef]
22. Gangopadhyay, A.; Robinson, A.R. Circulation and dynamics of the western north Atlantic. Part III: Forecasting the meanders and rings. *J. Atmos. Ocean. Technol.* **1997**, *14*, 1352–1365. [CrossRef]
23. Oram, J.; McWilliams, J.C.; Stolzenbach, K.D. Gradient-based edge detection and feature classification of sea-surface images of the Southern California Bight. *Remote Sens. Environ.* **2008**, *112*, 2397–2415. [CrossRef]
24. Ping, B.; Su, F.; Meng, Y.; Fang, S.; Du, Y. A model of sea surface temperature front detection based on a threshold interval. *Acta Oceanol. Sin.* **2014**, *33*, 65–71. [CrossRef]
25. Holyer, R.J.; Peckinpaugh, S.H. Edge detection applied to satellite imagery of the oceans. *IEEE Trans. Geosci. Remote* **1989**, *27*, 46–56. [CrossRef]
26. Yang, Y.; Dong, J.; Sun, X.; Lguensat, R.; Jian, M.; Wang, X. Ocean front detection from instant remote sensing SST images. *IEEE Geosci. Remote Sens. Lett.* **2016**, *13*, 1960–1964. [CrossRef]
27. Ullman, D.S.; Cornillon, P.C. Evaluation of front detection methods for satellite-derived SST data using in situ observations. *J. Atmos. Ocean. Technol.* **2000**, *17*, 1667–1675. [CrossRef]
28. Kahru, M.; Håkansson, B.; Rud, O.E. Distributions of the sea-surface temperature fronts in the Baltic Sea as derived from satellite imagery. *Cont. Shelf Res.* **1995**, *15*, 663–679. [CrossRef]
29. Moore, J.K.; Abbott, M.R.; Richman, J.G. Location and dynamics of the Antarctic Polar Front from satellite sea surface temperature data. *J. Geophys. Res.* **1999**, *104*, 3059–3073. [CrossRef]
30. Ullman, D.S.; Cornillon, P.C. Satellite-derived Sea surface temperature fronts on the continental shelf off the northeast U.S. coast. *J. Geophys. Res.* **1999**, *104*, 23459–23478. [CrossRef]
31. Ullman, D.S.; Cornillon, P.C. Continental shelf surface thermal fronts in winter off the northeast US coast. *Cont. Shelf Res.* **2001**, *21*, 1139–1156. [CrossRef]
32. Kostianoy, A.G.; Ginzburg, A.; Frankignoulle, M.; Delille, B. Fronts in the Southern Indian Ocean as inferred from satellite sea surface temperature data. *J. Mar. Syst.* **2004**, *45*, 55–73. [CrossRef]
33. Park, K.; Ullman, D.S.; Kim, K.; Chung, J.Y.; Kim, K. Spatial and temporal variability of satellite-observed Subpolar Front in the East/Japan Sea. *Deep Sea Res.* **2007**, *54*, 453–470. [CrossRef]
34. Hickox, R.C.; Belkin, I.M.; Cornillon, P.C.; Shan, Z. Climatology and seasonal variability of ocean fronts in the East China, Yellow and Bohai seas from satellite SST data. *Geophys. Res. Lett.* **2000**, *27*, 2945–2948. [CrossRef]
35. Wang, D.; Liu, Y.; Qi, Y.; Shi, P. Seasonal variability of thermal fronts in the northern South China Sea from satellite data. *Geophys. Res. Lett.* **2001**, *28*, 3963–3966. [CrossRef]
36. Chu, P.C.; Guihua, W. Seasonal variability of thermohaline front in the central South China Sea. *J. Oceanogr.* **2003**, *59*, 65–78. [CrossRef]
37. Chen, C.A. Chemical and physical fronts in the Bohai, Yellow and East China seas. *J. Mar. Syst.* **2009**, *78*, 394–410. [CrossRef]
38. Zhu, K.; Chen, X.; Mao, K.; Hu, D.; Hong, S.; Li, Y. Mixing characteristics of the subarctic front in the Kuroshio-Oyashio confluence region. *Oceanologia* **2019**, *61*, 103–113. [CrossRef]
39. Chen, Y.; Fan, R.; Bilal, M.; Yang, X.; Wang, J.; Li, W. Multilevel cloud detection for high-resolution remote sensing imagery using multiple convolutional neural networks. *ISPRS Int. J. Geo Inf.* **2018**, *7*, 181. [CrossRef]
40. Chen, Y.; Tang, L.; Kan, Z.; Bilal, M.; Li, Q. A novel water body extraction neural network (WBE-NN) for optical high-resolution multispectral imagery. *J. Hydrol.* **2020**, *588*, 125092. [CrossRef]
41. Reichstein, M.; Camps-Valls, G.; Stevens, B.; Jung, M.; Denzler, J.; Carvalhais, N.; Prabhat. Deep learning and process understanding for data-driven Earth system science. *Nature* **2019**, *566*, 195–204. [CrossRef]
42. Lima, E.B.; Sun, X.; Dong, J.; Wang, H.; Yang, Y.; Liu, L. Learning and transferring convolutional neural network knowledge to ocean front recognition. *EEE Geosci. Remote Sens. Lett.* **2017**, *14*, 354–358. [CrossRef]
43. Sun, X.; Wang, C.; Dong, J.; Lima, E.B.; Yang, Y. A multiscale deep framework for ocean fronts detection and fine-grained location. *IEEE Geosci. Remote Sens. Lett.* **2019**, *16*, 178–182. [CrossRef]
44. Li, Y.; Liang, J.; Da, H.; Chang, L.; Li, H. A deep learning method for ocean front extraction in remote sensing imagery. *IEEE Geosci. Remote Sens. Lett.* **2022**, *19*, 1–5. [CrossRef]
45. Li, Q.; Fan, Z.; Zhong, G. BEDNet: Bi-directional edge detection network for ocean front detection. *Iconip* **2020**, *1332*, 312–319. [CrossRef]

46. Lima, E.B.; Sun, X.; Yang, Y.; Dong, J. Application of deep convolutional neural networks for ocean front recognition. *J. Appl. Remote Sens.* **2017**, *11*, 1. [CrossRef]
47. Li, Q.; Zhong, G.; Xie, C. Hedjam, R. Weak edge identification network for ocean front detection. *IEEE Geosci. Remote Sens. Lett.* **2022**, *19*, 1–5. [CrossRef]
48. Xie, C.; Guo, H.; Dong, J. LSENet: Location and seasonality enhanced network for multi-class ocean front detection. *IEEE Trans. Geosci. Remote Sens.* **2022**, *60*, 1–9. [CrossRef]
49. Sun, J.; Zhong, G.; Dong, J.; Saeeda, H.; Zhang, Q. Cooperative profit random forests with application in ocean front recognition. *IEEE Access* **2017**, *5*, 1398–1408. [CrossRef]
50. Yang, Y.; Lam, K.; Sun, X.; Dong, J.; Lguensat, R. An efficient algorithm for ocean-front evolution trend recognition. *Remote Sens.* **2022**, *14*, 259. [CrossRef]
51. Mandelberg, M.D.; Frizzell-Makowski, L.J. Acoustic provincing of ocean basins. In Proceedings of the Oceans 2000 MTS/IEEE Conference and Exhibition, Providence, RI, USA, 11–14 September 2000; pp. 105–108. [CrossRef]
52. Wang, H.; Li, Y.; Li, Q.; Yu, X. Cluster analysis of deep-water sound speed profiles in Indian Ocean. *IOP Conf. Ser. Earth Environ. Sci.* **2019**, *310*, 052048. [CrossRef]
53. Abiva, J.; Fabbri, T.; Vicen-Bueno, R. Automatic classification of sound speed profiles using PCA and self-organizing map techniques. In Proceedings of the Oceans Marseille, Marseille, France, 17–20 June 2019; pp. 1–10. [CrossRef]
54. Dubberley, J.; Zingerelli, R. Fuzzy clustering of oceanographic sound speed profiles for acoustic characterization. *J. Acoust. Soc. Am.* **2008**, *123*, 8665–8669. [CrossRef]
55. Meredith, R.W.; Mensi, B.; Gendron, M.L. Hierarchical clustering of historic sound speed profiles. In Proceedings of the OCEANS 2008, Quebec City, QC, Canada, 15–18 September 2008; pp. 1–7. [CrossRef]
56. Liu, Y.; Chen, C. Clustering sound speed profiles in the East China Sea. In Proceedings of the 2018 OCEANS - MTS/IEEE Kobe Techno-Oceans (OTO), Kobe, Japan, 28–31 May 2018; pp. 1–4. [CrossRef]
57. Liu, Y.; Chen, W.; Chen, W.; Chen, Y.; Ma, L.; Meng, Z. Sound field distribution characteristics of typical Kuroshio Front in different seasons. In Proceedings of the 2021 4th International Conference on Information Communication and Signal Processing (ICICSP), Shanghai, China, 24–26 September 2021; pp. 219–223. [CrossRef]
58. Liu, Y.; Chen, W.; Chen, W.; Chen, Y.; Ma, L.; Meng, Z. Reconstruction of ocean front model based on sound speed clustering and its effectiveness in ocean acoustic forecasting. *Appl. Sci.* **2021**, *11*, 8461. [CrossRef]
59. Liu, Y.; Chen, W.; Chen, W.; Chen, Y.; Ma, L.; Meng, Z. Reconstruction method of ocean front model based on fuzzy cluster analysis of sound speed profile. *IEEE Access* **2021**, *9*, 112714–112725. [CrossRef]
60. Liu, Y.; Chen, W.; Chen, Y.; Chen, W.; Ma, L.; Meng, Z. Ocean front reconstruction method based on K-means algorithm iterative hierarchical clustering sound speed profile. *J. Mar. Sci. Eng.* **2021**, *9*, 1233. [CrossRef]
61. Gangopadhyay, A.; Robinson, A.R. Feature oriented regional modeling of oceanic fronts. *Dyn. Atmos. Ocean* **2002**, *36*, 201–232. [CrossRef]
62. Gangopadhyay, A.; Robinson, A.R.; Haley, P.J.; Leslie, W.G.; Yu, Z. Feature-oriented regional modeling and simulations in the Gulf of Maine and Georges Bank. *Cont. Shelf Res.* **2003**, *23*, 317–353. [CrossRef]
63. Carriere, O.; Hermand, J.P. Feature-oriented acoustic tomography for coastal ocean observatories. *IEEE J. Ocean. Eng.* **2013**, *38*, 534–546. [CrossRef]
64. Smeed, D.A.; Alderson, S.G. Inference of deep ocean structure from upper-ocean measurements. *J. Atmos. Ocean Technol.* **1997**, *14*, 604–615. [CrossRef]
65. Wilson, W.D. Equation for the speed of sound in seawater. *J. Acoust. Soc. Am.* **1960**, *32*, 1357. [CrossRef]
66. Rousseau, T.H.; Siegmann, W.L.; Jacobson, M.J. Acoustic propagation through a model of shallow fronts in the deep ocean. *J. Acoust. Soc. Am.* **1982**, *72*, 924–936. [CrossRef]
67. Rousseau, T.H.; Jacobson, M.J.; Siegmann, W.L. Shallow-ocean fronts: Effects on array performance and acoustic prediction of properties. *J. Acoust. Soc. Am.* **1983**, *74*, S97. [CrossRef]
68. De Courcy, B.J.; Lin, Y.; Siegmann, W.L. Effects of front width on acoustic ducting by a continuous curved front over a sloping bottom. *J. Acoust. Soc. Am.* **2019**, *146*, 1923. [CrossRef]
69. Liu, Y.; Chen, W.; Chen, W.; Chen, Y.; Ma, L.; Meng, Z. Ocean front model based on sound speed profile and its influence on sound propagation. In Proceedings of the 2021 OES China Ocean Acoustics (COA), Harbin, China, 14–17 July 2021; pp. 172–177. [CrossRef]
70. Lin, Y.; Newhall, A.E.; Lynch, J.F. Impact of a shelfbreak front on array processing in shallow water. *J. Acoust. Soc. Am.* **2007**, *121*, 3203. [CrossRef]
71. Weinberg, N.L.; Clark, J.G. Horizontal acoustic refraction through ocean mesoscale eddies and fronts. *J. Acoust. Soc. Am.* **1980**, *68*, 703–705. [CrossRef]
72. Mellberg, L.E.; Johannessen, O.M.; Connors, D.N.; Botseas, G.; Browning, D.G. Acoustic propagation in the western Greenland Sea frontal zone. *J. Acoust. Soc. Am.* **1991**, *89*, 2144–2156. [CrossRef]
73. Shapiro, G.I.; Chen, F.; Thain, R. The effect of ocean fronts on acoustic wave propagation in the Celtic Sea. *J. Mar. Syst.* **2014**, *139*, 217–226. [CrossRef]

74. Lynch, J.F.; Newhall, A.E.; Sperry, B.J.; Gawarkiewicz, G.G.; Fredricks, A.; Tyack, P.L.; Chiu, C.; Abbot, P.A. Spatial and temporal variations in acoustic propagation characteristics at the New England shelfbreak front. *IEEE J. Ocean. Eng.* **2003**, *28*, 129–150. [CrossRef]
75. Ramp, S.R.; Chiu, C.; Bahr, F.; Qi, Y.; Dahl, P.H.; Miller, J.F.; Lynch, J.F.; Zhang, R.; Zhou, J. The shelf-edge frontal structure in the central East China Sea and its impact on low-frequency acoustic propagation. *IEEE J. Ocean. Eng.* **2004**, *29*, 1011–1031. [CrossRef]
76. Moore, K.A.; Miller, J.H.; Potty, G.R.; Lynch, J.F.; Newhall, A.E. Investigation of three-dimensional propagation effects at the New Jersey shelf break front. *J. Acoust. Soc. Am.* **2007**, *121*, 3126. [CrossRef]
77. Deferrari, H.A. Effects of offshore mesoscale eddies and fronts on inshore shallow water acoustic propagation. *J. Acoust. Soc. Am.* **2007**, *122*, 3006. [CrossRef]
78. Moore, K.A.; Miller, J.H.; Potty, G.R.; Dossot, G.A.; Glenn, S.; Lynch, J.F. Measurements of 3-D propagation effects at a shelfbreak front. *J. Acoust. Soc. Am.* **2006**, *120*, 3222. [CrossRef]
79. Jensen, F.B.; Dreini, G.; Prior, M.K. Acoustic effects of the Iceland-Faeroe Front. In *Ocean Variability & Acoustic Propagation*; Potter, J., Warn-Varnas, A., Eds.; Springer: New York, NY, USA, 1991. [CrossRef]
80. Kravchun, P.N. Influence of the benthic front on the mode structure of acoustic field in the ocean. *Acoust. Phys.* **2008**, *54*, 371–374. [CrossRef]
81. Chiu, C.; Lynch, J.F.; Gawarkiewicz, G.G. Shallow-water tomography: Acoustic maps of the New England shelfbreak front. *J. Acoust. Soc. Am.* **1999**, *105*, 1176. [CrossRef]
82. Xuehong, Z.; Xinzhong, L. A numerical world ocean general circulation model. *Adv. Atmos. Sci.* **1989**, *6*, 44–61. [CrossRef]
83. Shu, Q.; Qiao, F.; Song, Z.; Yin, X. A comparison of two global ocean-ice coupled models with different horizontal resolutions. *Acta Oceanol. Sin.* **2013**, *32*, 1–11. [CrossRef]
84. Dongarra, J.J.; Beckman, P.H.; Moore, T.L.; Aerts, P.; Aloisio, G.; André, J.; Barkai, D.; Berthou, J.; Boku, T.; Braunschweig, B.; et al. The international exascale software project roadmap. *Int. J. High Perform. Comput. Appl.* **2011**, *25*, 3–60. [CrossRef]
85. Sun, Z.; Sandoval, L.; Crystal-Ornelas, R.; Mousavi, S.M.; Wang, J.; Lin, C.; Cristea, N.C.; Tong, D.Q.; Carande, W.H.; Ma, X.; et al. A review of Earth Artificial Intelligence. *Comput. Geosci.* **2022**, *159*, 105034. [CrossRef]
86. Semtner, A.; Chervin, R. Ocean general circulation from a global eddy-resolving model. *J. Geophys. Res.* **1992**, *97*, 5493–5550. [CrossRef]
87. Parsons, A.R.; Bourke, R.H.; Muench, R.D.; Chiu, C.; Lynch, J.F.; Miller, J.H.; Plueddemann, A.J.; Pawlowicz, R. The Barents Sea Polar Front in summer. *J. Geophys. Res.* **1996**, *101*, 14201–14221. [CrossRef]
88. Apel, J.R.; Badiey, M.; Chiu, C.; Finette, S.; Headrick, R.H.; Kemp, J.N.; Lynch, J.F.; Newhall, A.E.; Orr, M.H.; Pasewark, B.H.; et al. An overview of the 1995 SWARM shallow-water internal wave acoustic scattering experiment. *IEEE J. Ocean. Eng.* **1997**, *22*, 465–500. [CrossRef]
89. Duda, T.F.; Lynch, J.F.; Newhall, A.E.; Wu, L.; Chiu, C. Fluctuation of 400-Hz sound intensity in the 2001 ASIAEX South China Sea experiment. *IEEE J. Ocean. Eng.* **2004**, *29*, 1264–1279. [CrossRef]
90. Wang, N.; Liu, J.; Gao, D.; Gao, W.; Wang, H.Z. An overview of the 2005 YFIAE: Yellow Sea oceanic front and internal waves acoustic experiment. *J. Acoust. Soc. Am.* **2008**, *124*, 2444. [CrossRef]
91. Tang, D.; Moum, J.N.; Lynch, J.F.; Abbot, P.A.; Chapman, R.; Dahl, P.H.; Duda, T.F.; Gawarkiewicz, G.G.; Glenn, S.; Goff, J.A.; et al. Shallow Water '06: A joint acoustic propagation/nonlinear internal wave physics experiment. *Oceanography* **2007**, *20*, 156–167. [CrossRef]
92. Flatteé, S.M.; Duda, T.F.; Colosi, J.A.; Hildebrand, J.A.; Hodgkiss, W.S.; Worcester, P.F.; Cornuelle, B.D.; Howe, B.; Mercer, J.A.; Spindel, R.C.; et al. Wave-front fluctuations in the 1000-km SLICE89 experiment. *J. Acoust. Soc. Am.* **1991**, *89*, 1962. [CrossRef]
93. Dzieciuch, M.A.; Vera, M.D.; Colosi, J.A.; Cornuelle, B.D.; Dushaw, B.; Howe, B.; Mercer, J.A.; Munk, W.H.; Spindel, R.C.; Worcester, P.F. Horizontal coherence of tracked arrivals in the North Pacific Acoustic Laboratory98 (NPAL98). *J. Acoust. Soc. Am.* **2006**, *120*, 3022. [CrossRef]
94. Brown, M.G.; Colosi, J.A.; Virovlyansky, A.L.; Zaslavsky, G.; Tomsovic, S.; Wolfson, M.A. Ray dynamics in the AET experiment. *J. Acoust. Soc. Am.* **2000**, *108*, 2578. [CrossRef]
95. Heaney, K.D. Internal wave strength inversion and localization using long-range acoustic signals. *J. Acoust. Soc. Am.* **1997**, *102*, 3142. [CrossRef]
96. Mercer, J.A.; Colosi, J.A.; Howe, B.M.; Dzieciuch, M.A.; Stephen, R.; Worcester, P.F. LOAPEX: The long-range ocean acoustic propagation experiment. *IEEE J. Ocean. Eng.* **2009**, *34*, 1–11. [CrossRef]
97. Wage, K.E.; Farrokhrooz, M.; Dzieciuch, M.A.; Worcester, P.F. Analysis of the vertical structure of deep ocean noise using measurements from the SPICEX and PhilSea experiments. *J. Acoust. Soc. Am.* **2013**, *133*, 070041. [CrossRef]